Uniaxial Compression Testing

Howard A. Kuhn, Concurrent Technologies Corporation

Introduction

COMPRESSION LOADS occur in a wide variety of material applications, such as steel building structures and concrete bridge supports, as well as in material processing, such as during the rolling and forging of a billet. Characterizing the material response to these loads requires tests that measure the compressive behavior of the materials. Results of these tests provide accurate input parameters for product-or process-design computations.

Under certain circumstances, compression testing may also have advantages over other testing methods. Tension testing is by far the most extensively developed and widely used test for material behavior, and it can be used to determine all aspects of the mechanical behavior of a material under tensile loads, including its elastic, yield, and plastic deformation and its fracture properties. However, the extent of deformation in tension testing is limited by necking. To understand the behavior of materials under the large plastic strains during deformation processing, measurements must be made beyond the tensile necking limit. Compression tests and torsion tests are alternative approaches that overcome this limitation.

Furthermore, compression-test specimens are simpler in shape, do not require threads or enlarged ends for gripping, and use less material than tension-test specimens. Therefore, compression tests are often useful for subscale testing and for component testing where tension-test specimens would be difficult to produce. Examples of these applications include through-thickness property measurements in plates and forgings (Ref 1), weld heat-affected zones, and precious metals (Ref 2) where small amounts of material are available.

In addition, characterizing the mechanical behavior of anisotropic materials often requires compression testing. For isotropic polycrystalline materials, compressive behavior is correctly assumed to be identical to tensile behavior in terms of elastic and plastic deformation. However, in highly textured materials that deform by twinning, as opposed to dislocation slip, compressive and tensile deformation characteristics differ widely (Ref 3). Likewise, the failure of unidirectionally reinforced composite materials, particularly along the direction of reinforcement, is much different in compression than in tension.

In this article, the characteristics of deformation during axial compression testing are described, including the deformation modes, compressive properties, and compression-test deformation mechanics. Procedures are described for the use of compression testing for measurement of the deformation properties and fracture properties of materials.

References cited in this section

1. T. Erturk, W.L. Otto, and H.A. Kuhn, Anisotropy of Ductile Fracture—An Application of the Upset Test, *Metall. Trans*., Vol 5, 1974, p 1883

2. W.A. Kawahara, Tensile and Compressive Materials Testing with Sub-Sized Specimens, *Exp. Tech*., Nov/Dec, 1990, p 27–29

3. W.A. Backofen, *Deformation Processing*, Addison-Wesley, Reading, MA, p 53

Deformation Modes in Axial Compression

Compression tests can provide considerable useful information on plastic deformation and failure, but certain precautions must be taken to assure a valid test of material behavior. Figure 1 illustrates the modes of deformation that can occur in compression testing. The buckling mode shown in Fig. 1(a) occurs when the length-to-width ratio of the test specimen is very large, and can be treated by classical analyses of elastic and plastic buckling (Ref 4). These analyses predict that cylindrical specimens having length-to-diameter ratios,*L* /*D*, less than 5.0 are safe from buckling and can be used for compression testing of brittle and ductile materials. Practical experience with ductile materials, on the other hand, shows that even *L*/*D* ratios as low as 2.5 lead to unsatisfactory deformation responses. For these geometries, even slightly eccentric loading or nonparallel compression plates will lead to shear distortion, as shown in Fig. 1(b). Therefore, *L*/*D* ratios less than 2.0 are normally used to avoid buckling and provide accurate measurements of the plastic deformation behavior of materials in compression.

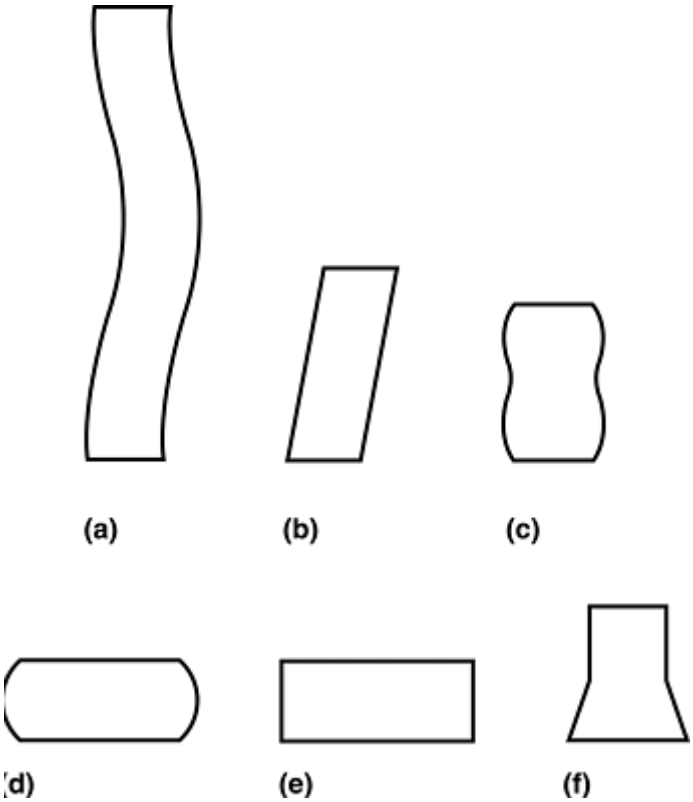

Fig. 1 Modes of deformation in compression. (a) Buckling, when *L*/*D* > 5. (b) Shearing, when*L*/*D* > 2.5. (c) Double barreling, when*L*/*D* > 2.0 and friction is present at the contact surfaces. (d) Barreling, when *L*/*D* < 2.0 and friction is present at the contact surfaces. (e) Homogenous compression, when *L*/*D* < 2.0 and no friction is present at the contact surfaces. (f) Compressive instability due to work-softening material

Friction is another source of anomalous deformation in compression testing of ductile materials. Friction between the ends of the test specimen and the compression platens constrains lateral flow at the contact surfaces, which leads to barreling or bulging of the cylindrical surface. Under these circumstances, for *L*/*D* ratios on the order of 2.0, a double barrel forms, as shown in Fig. 1(c), smaller *L*/*D* ratios lead to a single barrel, as in Fig. 1(d). Barreling indicates that the deformation is nonuniform (i.e., the stress and strain vary throughout the test specimen), and such tests are not valid for measurement of the bulk elastic and plastic properties of a material. Barreling, however, can be beneficial for the measurement of the localized fracture properties of a material, as described in the section "Instability in Compression" of this article.

If the compression test can be carried out without friction between the specimen and compression platens, barreling does not occur, as shown in Fig. 1(e), and the deformation is uniform (homogenous). For measurement of the bulk deformation properties of materials in compression, this configuration must be achieved.

A final form of irregular deformation in axial compression is an instability that is the antithesis of necking in tension. In this case, the instability occurs due to work softening of the material and takes the form of rapid, localized expansion, as shown in Fig. 1(f).

Reference cited in this section

4. J.H. Faupel and F.E. Fisher, *Engineering Design*, John Wiley & Sons, 1981, p 566–592

Uniaxial Compression Testing

Howard A. Kuhn, Concurrent Technologies Corporation

Compressive Properties

The bulk elastic and plastic deformation characteristics of polycrystalline materials are generally the same in compression and tension. As a result, the elastic-modulus, yield-strength, and work-hardening curves will be the same in compression and tension tests. Fracture strength, ultimate strength, and ductility, on the other hand, depend on localized mechanisms of deformation and fracture, and are generally different in tension and compression testing. Anisotropic materials, such as composite materials and highly textured polycrystalline materials, also exhibit considerable differences between tensile and compressive behaviors beyond initial elastic response.

Measurements of bulk elastic modulus and yield strength require accurate measurements of the axial strain of the material under compression testing. This is accomplished by attaching to the specimen an extensometer, which uses a differential transformer or strain gages to provide an electronic signal that is proportional to the displacement of gage marks on the specimen. Extensometers are most easily used in tension testing because tension test specimens are long and provide ample space for attachment of the extensometer clips. Due to the limitations noted in the previous section (Fig. 1a and b), compression-test specimens are considerably smaller in length and make attachment of the extensometer clips difficult. Alternatively, a differential transformer can be used to measure the displacement between the compression platen surfaces. Because the measurement is not made directly on the specimen, however, elastic distortion and slight rotations of the platens during testing will give false displacement readings.

Measurement of the work-hardening, or plastic-flow, curve of a material is best carried out by compression testing, particularly if the application, such as bulk metalworking, requires knowledge of the flow behavior at large plastic strains beyond the necking limit in tension testing. In this case, the strains are many orders of magnitude larger than the elastic strains, and indirect measurement of the axial strain by monitoring the motion of the compression platens is sufficiently accurate. Any systematic errors caused by elastic deformation of the platens or test equipment are insignificant compared to the large plastic displacements of the compression specimen.

The fracture strength of a material is much different in tension and compression. In tension, the fracture strength of a ductile material is determined by its necking behavior, which concentrates the plastic deformation in a small region, generates a triaxial stress state in the neck region, and propagates ductile fracture from voids that initiate at the center of the neck region. The fracture strength of a brittle material in tension, on the other hand, is limited by its cleavage stress.

In compression of a ductile material, necking does not occur, so the void generation and growth mechanism that leads to complete separation in the tension test does not terminate the compression test. Ductile fractures can form, however, on the barreled surface of a compression specimen with friction. These fractures generally grow slowly and do not lead to complete separation of the specimen, so the load-carrying capacity of the material is not limited. As a result, there is no definition of fracture strength in compression of ductile materials. Surface cracks that may form on the barreled surface of compression tests with friction depend not only on the material,

but also on the amount of friction and the *L*/*D* ratios of the specimen, as described in the section “Compression Testing for Ductile Fracture” in this article.

In compression of a brittle or low-ductility material, however, fracture occurs catastrophically by shear. The failure either occurs along one large shear plane, leading to complete separation, or at several sites around the specimen, leading to crushing of the material. In either case, the load-carrying capacity of the material comes to an abrupt halt, and the fracture strength of the material is easily defined as the load at that point divided by the cross-sectional area.

The ultimate strength of a material in tension is easily defined as the maximum load-bearing capacity. In a ductile material, this occurs at the initiation of necking. In a brittle material, it occurs at fracture. Because necking does not occur in compression testing, there is no ultimate compressive strength in ductile materials, and in brittle materials the ultimate compressive strength occurs at fracture. The only exception to this is in materials that exhibit severe work softening, in which case, plastic instability (Fig. 1f) leads to an upper limit in load-carrying capacity, which defines the ultimate strength of the material, as described in the section "Instability in Compression" in this article.

Uniaxial Compression Testing

Howard A. Kuhn, Concurrent Technologies Corporation

Plasticity Mechanics

Further understanding of the axial compression test can be obtained by examining the interactions between the plastic flow and forces acting during the test. The essential features of this interaction can be developed by considering a thin, vertical slab of material in a compression-test specimen (Fig. 2a). Pressure, *P*, from the compression platens acts on the top and bottom of the slab. Because this slab is to the right of the centerline, the slab moves to the right as the compression test progresses. Motion of the slab to the right, coupled with the pressure from the platens, causes friction, *f*, on the top and bottom surfaces of the slab. The direction of friction on the slab is to the left, opposing the motion of the slab.

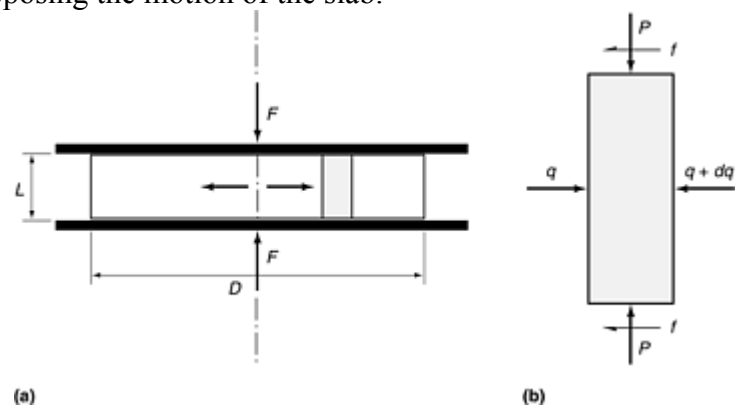

Fig. 2 Interactions between plastic flow and forces acting during compression testing. (a) Schematic of a compression test showing applied force *F*, radial expansion away from the centerline, and a slab element of material in a compression test. (b) Forces acting on the slab. *P*, pressure from the compression platens; *f*, friction at the contract surfaces, acting opposite to motion of the slab; *q*, internal radial pressure in the test specimen

Extracting the slab from the compression test, shown in Fig. 2(b), it is clear that the friction forces on the top and bottom of the slab cause an imbalance of forces in the horizontal direction. This implies that there must be internal horizontal forces acting on the vertical faces of the slab to maintain force equilibrium (forces due to acceleration are negligible). As shown in Fig. 2(b), the resulting horizontal pressure, *q*, acting on opposite sides of the slab must differ by some amount, *dq*, to achieve equilibrium.

Applying the principle of equilibrium to the slab in the horizontal direction gives a simple differential equation for the horizontal pressure q:

$$dq/dr = -2f/L \quad \text{(Eq 1)}$$

where L is the thickness of the compression-test specimen. At the outside edge of the test specimen ($r = D/2$), the horizontal pressure must be zero (free surface); therefore, Eq 1 shows that q increases from zero at the edge to positive values inside the test specimen. Furthermore, Eq 1 shows that the rate of increase of q toward the centerline is larger for high values of friction and low values of specimen thickness. If f is constant, the internal pressure distribution is:

$$q = f(D/L)(1 - 2r/D) \quad \text{(Eq 2)}$$

which has a peak value at $r = 0$.

Finally, the vertical pressure, P, is related to the internal pressure, q, by the yield criterion for plastic deformation:

$$P = q + \sigma_0 \quad \text{(Eq 3)}$$

where σ_0 is the yield strength of the material. Therefore, P has the same distribution as the radial stress, q, plus the material yield strength. Integrating this pressure distribution over the contact area gives the total force, F.

Schematic plots of the pressure distribution, P, in axial compression are given in Fig. 3. Note that even though the deformation is uniform at every point, the compressive stress is not uniform, but reaches peak values at the centerline. The values of this peak pressure increase as friction increases and as the test specimen aspect ratio, L/D, decreases. More importantly, if friction is zero, Eq 2 shows that internal pressure, q, is zero throughout the test specimen. Then, from Eq 3, P is uniform and equal to σ_0. Frictionless conditions, therefore, must be used to measure the plastic deformation response of a material, as described in the next section. More detailed analysis of the plasticity mechanics of axial compression are given in Ref 5.

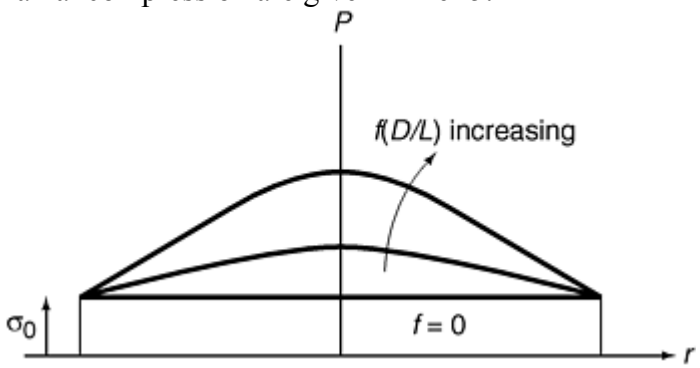

Fig. 3 Schematic of pressure distributions, *P*, in a compression test. When friction is zero, *P* is uniform and equal to the material flow stress, σ_0, but increasing friction and decreasing*L*/*D* with friction lead to increasingly nonuniform pressure distributions with peak values at the centerline.

The analysis given above is strictly valid only for specimens having very low aspect ratios. However, the essential roles of friction and geometry are valid qualitatively for test specimens having large aspect ratios; for these test specimens, the deformation patterns are very complex and vary in the thickness direction, as well as in the lateral direction. A macrograph of a compression test cross section, shown in Fig. 4(a), reveals the nonuniformity of internal deformation patterns due to friction at the contact surfaces. In general, the internal deformation depicted in Fig. 4(b) can be described as three zones (Ref 6): (a) nearly undeformed wedges at the top and bottom (referred to as dead-metal zones), (b) crisscrossing regions of intense shear deformation, and (c) moderately deformed regions near the barrel surfaces. The severity of barreling and the differences in degree of deformation between the three regions increase as friction at the contact surfaces increases.

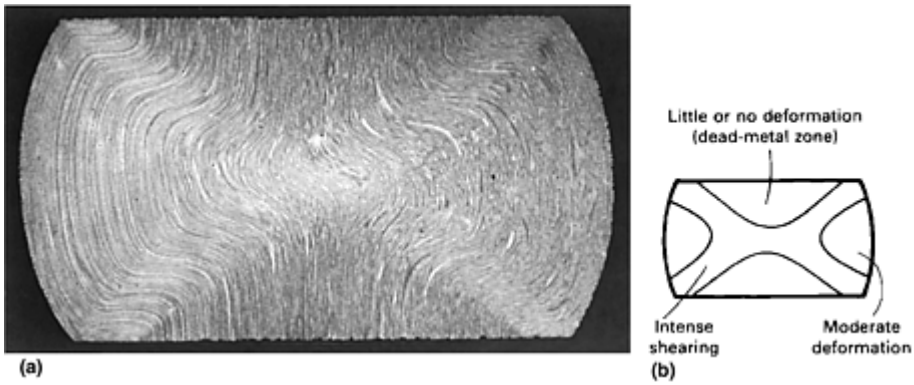

Fig. 4 Internal deformation in compression testing. (a) Macrograph of the internal deformation in a compression-test specimen with high-contact surface friction. Source: Ref 5. (b) Schematic representation of the internal deformation into three zones. I, nearly undeformed wedges at the contact surfaces (dead-metal zones); II, criss-crossing regions of intense shear deformation; III, moderately deformed regions near the bulge surface. Source: Ref 6

References cited in this section

5. G.E. Dieter, *Mechanical Metallurgy*, 2nd ed., McGraw-Hill, 1976, p 561–565

6. G.E. Dieter, Evaluation of Workability: Introduction, *Forming and Forging*, Vol 14, *ASM Handbook,* ASM International, 1988, p 365

Uniaxial Compression Testing

Howard A. Kuhn, Concurrent Technologies Corporation

Homogenous Compression for Plastic Deformation Behavior

Under homogenous-compression conditions (frictionless compression), height reduction and the resulting radial and circumferential expansion are uniform throughout the test specimen. Furthermore, under these conditions, radial and circumferential stresses are zero, and the only stress acting is the uniform compressive stress in the axial direction, as described in the previous section.

Homogenous compression is accomplished by eliminating friction at the contact surfaces, which obviously requires the use of lubricants. Polishing the ends of the compression-test specimens as well as the die platens provides smooth surfaces, and lubricants applied to the contact surfaces form a low-friction layer between these surfaces. However, during compression of high-strength materials, the interface pressure between the test specimen and die platens becomes extremely high, and the lubricant squeezes out, leaving metal-on-metal contact, resulting in high friction.

One approach to retaining lubricants at the contact surface involves machining concentric circular grooves into the end faces of the test specimen (Fig. 5a) (Ref 7). Another approach was pioneered by Rastegaev and refined by Herbertz and Wiegels (Ref 8), in which the entire end face is machined away except for a small rim, as shown in Fig. 5(b). This traps a small volume of lubricant in the cavity, forming a hydrostatic cushion with nearly zero friction. This approach was modified by machining a tapered recess, as shown in Fig. 5(c), which reduces the amount of material removed and diminishes the strain measurement error. Furthermore this lubricant recess provides greater lubrication at the rim where material movement is greatest. During compression testing, radial displacement of the test material is zero at the center and increases linearly to the

outer rim. Evaluations of lubrication practice for high- temperature testing have shown that the tapered lubricant reservoir shown in Fig. 5(c) leads to the greatest reproducibility (Ref 9).

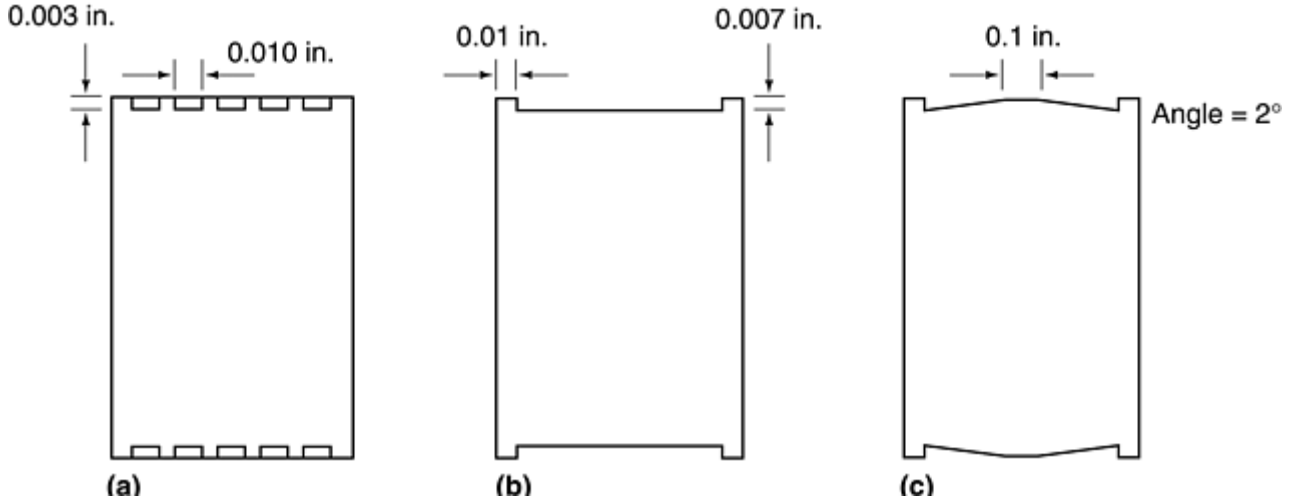

Fig. 5 Compression-test end profiles for lubricant entrapment. (a) Concentric grooves. Source: Ref 7. (b) Rastegaev reservoir. Source: Ref 8. (c) Modified Rastegaev reservoir. Source: Ref 9

Several high-pressure lubricants are available for room-temperature compression tests, including mineral oil, palm oil, stearates, and molybdenum disulfide. Teflon (E.I. DuPont de Nemours & Co., Inc., Wilmington, DE) in the form of spray or sheet is also widely used at room temperature and can be used at temperatures up to 500 °C (930 °F). For high-temperature testing of steels, titanium, and superalloys, one can use emulsions of graphite, molybdenum disulfide, and various glasses. It is important to match the grade of glass and resulting viscosity with the test temperature.

In homogenous compression tests, the plastic stress-strain curve can be easily calculated by measurement of the load, cross-sectional area, and height of the specimen throughout the test. The test can be conducted incrementally at room temperature wherein the specimen height and lateral dimensions are measured after each increment of deformation. For high-temperature deformation or continuous testing, the test-equipment load cell and crosshead displacement can be used to determine the load and dimensional changes of the specimen. In the latter measurement, it is necessary to remove systematic errors by first carrying out the compression test with no test specimen in place. This provides a load-stroke curve for the test-machine load train and measures the compliance of the various elements in the loaded column. Subtracting this compliance from the measured crosshead stroke during a compression test then provides a more accurate measurement of the specimen deformation. In any event, if constancy of volume can be assumed for the material being tested, then the cross-sectional area can be readily calculated from the specimen height at any point throughout the test.

References cited in this section

7. J.E. Hockett, The Cam Plastometer, in *Mechanical Testing*, Vol 8, *ASM Handbook*, ASM International, 1985, p 197

8. R. Herbertz and H. Wiegels, Ein Verfahren Zur Verwirklichurg des Reibungsfreien Zylinderstanch versuchs für die Ermittlung von Fliesscurven, *Stahl Eisen*, Vol 101, 1981, p 89–92

9. K. Lintermanns Fander, "The Flow and Fracture of Al-High Mg-Mn Alloys at High Temperatures and Strain Rates," Ph.D. dissertation, University of Pittsburgh, 1984, p 258

Compression Testing for Ductile Fracture

When friction exists at the die contact surfaces, material at the contact surfaces is retarded from moving outward while the material at the midplane is not constrained. As a result, barreling occurs, as shown in Fig. 1(c) and 1(d). Under these conditions, for a given axial compressive strain, the bulge profile provides circumferential strain at the equator that is greater than the strain that occurs during homogenous compression. At the same time, due to the bulge profile, the local compressive strain at the equator is less than the strain that would have occurred during homogenous compression for the same overall height strain. These surface strain deviations from homogenous compression increase as bulging increases; the severity of the bulge, in turn, is controlled by the magnitude of friction and the *L*/*D* ratio of the specimen. Figure 6 illustrates the progressive change in strain at the bulge surface for different lubrication and *L*/*D* ratios (Ref 10).

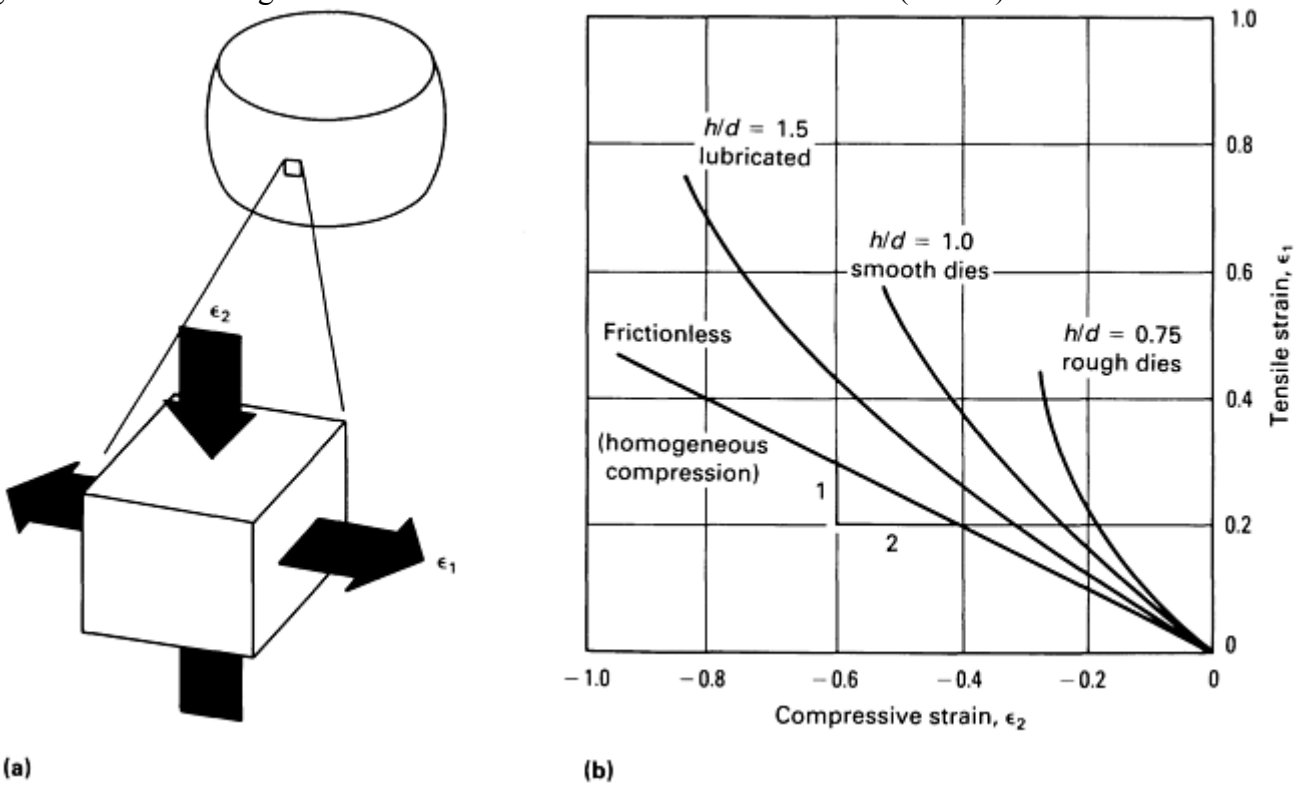

Fig. 6 Progressive change in strain at the bulge surface in compression testing. (a) Strains at the bulge surface of a compression test. (b) Variation of the strains during a compression test without friction (homogenous compression) and with progressively higher levels of friction and decreasing aspect ratio *L*/*D* (shown as *h*/*d*)

These strain combinations lead to tensile stress around the circumference and reduced compressive stress at the bulge equator. Therefore, compression tests with friction, and consequent bulging, can be used as tests for fracture. Figure 7 shows compression-test specimens with and without friction. Note that the compression test with the bulge surface, that is, with friction at the contact surfaces, has a crack caused by the tensile stress in the circumferential direction at the bulge surface. The homogenous compression specimen, even after greater height compression, has not bulged; therefore, there is no tensile stress in the circumferential direction, and the specimen has not cracked.

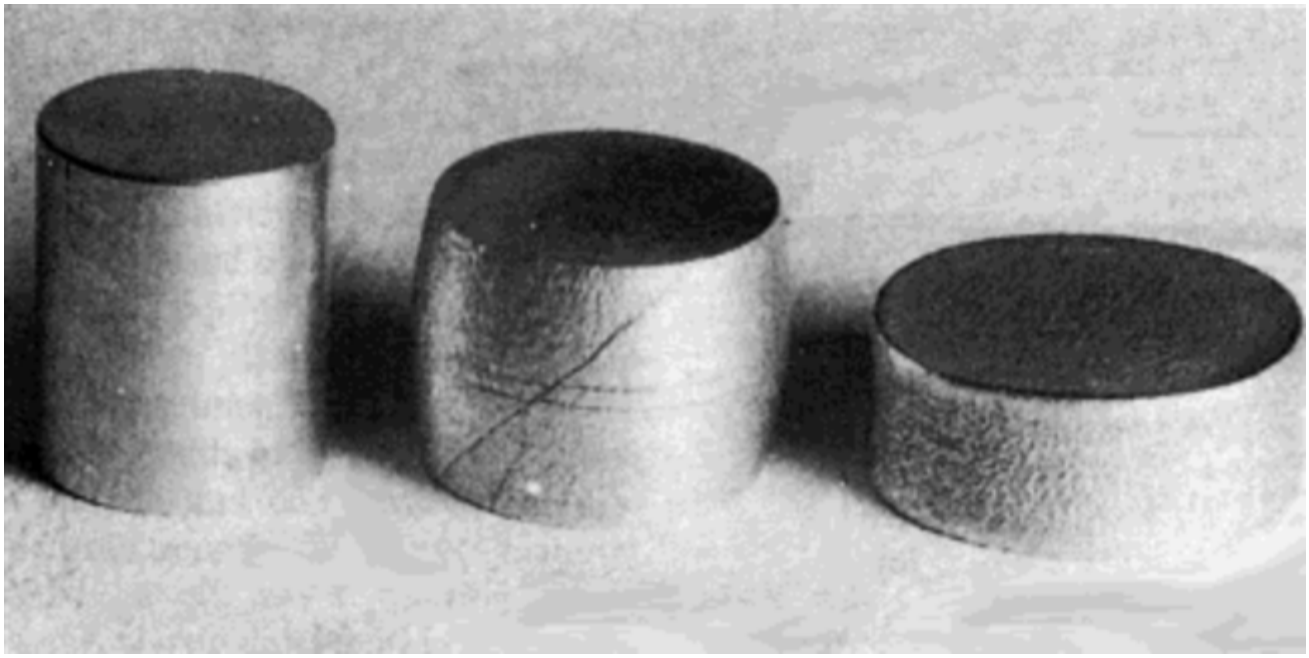

Fig. 7 Compression tests on 2024-T35 aluminum alloy. Left, undeformed specimen; center, compression with friction (cracked); right, compression without friction (no cracks)

The stress and strain environment at the bulge surface of upset cylinders suggests that axial compression tests can be used for workability measurements by carrying out the tests under a variety of conditions regarding interface friction and *L*/*D* ratios. By plotting the surface strains at fracture for each condition, a fracture strain locus can be generated representing the workability of the material. Figure 8 illustrates such a fracture locus. Modifications of the cylindrical compression-test specimen geometry have been used to enhance the range of strains over which fracture can be measured (Ref 11).

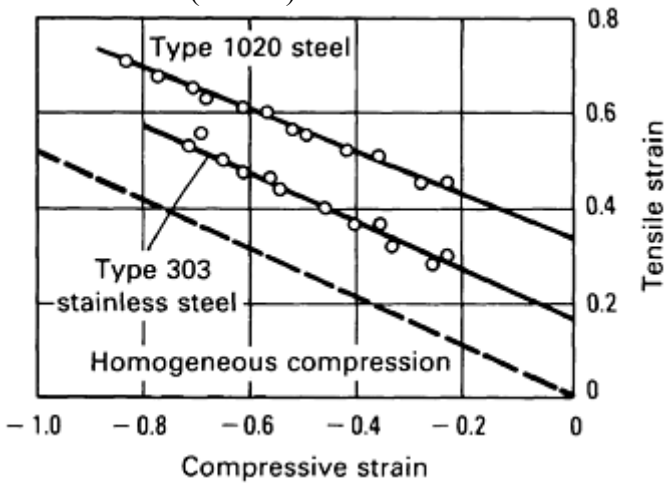

Fig. 8 Locus of fracture strains (workability) determined from compression test with friction. Source: Ref 10

References cited in this section

10. H.A. Kuhn, P.W. Lee, and T. Erturk, A Fracture Criterion for Cold Forging, *J. Eng. Mater. Technol. (Trans. ASME)*, Vol 95, 1973, p 213–218

11. H.A. Kuhn, Workability Theory and Application in Bulk Forming Processes, *Forming and Forging*, Vol 14, *ASM Handbook*, ASM International, 1988, p 389–391

Howard A. Kuhn, Concurrent Technologies Corporation

Instability in Compression

In tension testing, the onset of necking indicates unstable flow, characterized by a rapid decrease in diameter localized to the neck region. Up to this point, as the test specimen elongates, work hardening of the material compensates for the decrease in cross-sectional area; therefore, the material is able to carry an increasing load. However, as the work-hardening rate decreases, the flow stress acting across the decreasing cross-sectional area is no longer able to support the applied axial load. At this point, necking begins and the rate of decrease of cross-sectional area exceeds the rate of increase of work hardening, leading to instability and a rapidly falling tensile load as the neck progresses toward fracture.

In compression testing, a similar phenomenon occurs when work softening is prevalent (Ref 12). That is, during compression, the cross-sectional area of the specimen increases, which increases the load-carrying capability of the material. However, if work softening occurs, its load-carrying capability is decreased. When the rate of decrease in strength of the material due to work softening exceeds the rate of increase in the area of the specimen, an unstable mode of deformation occurs in which the material rapidly spreads in a localized region, as shown in Fig. 1(f).

Instability in tension and compression can be described through the Considére construction. Instability occurs when the slope of the load-elongation curve becomes zero, that is:

$$dF = d(\sigma A) = \sigma dA + A d\sigma = 0$$

or

$$d\sigma/\sigma = -dA/A = d\varepsilon = de/(1 + e)$$

and

$$d\sigma/de = \sigma/(1 + e) \qquad \text{(Eq 4)}$$

where σ is true stress, ε is true strain, e is engineering strain, F is force, and A is area.

Equation 4 indicates that instability occurs when the slope of the true stress-engineering strain curve equals the ratio of true stress to one plus the engineering strain. This leads to the Considére construction for instability (Fig. 9). The upper part of Fig. 9 shows the Considére construction for a tension test. When the work hardening stress-strain curve reaches point C, necking begins and unstable deformation continues through to complete separation or fracture. This defines the ultimate strength of the material in tension. In the lower part of Fig. 9, the Considére construction for the compression test shows that, for a work softening material, unstable flow commences at point C', leading to a configuration as shown in Fig. 1(f). Thus, the ultimate strength of the material in compression in this case can be defined as the stress at this point.

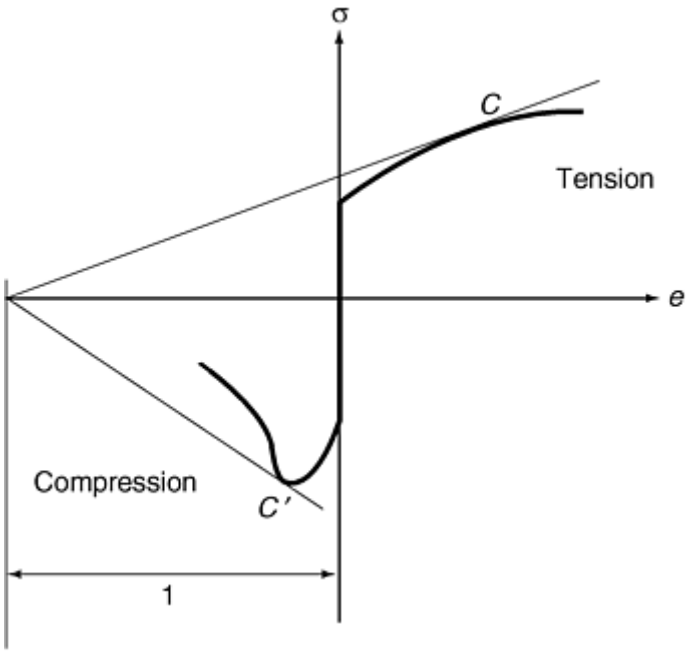

Fig. 9 Considére construction showing instability conditions in tension testing (due to decreasing work-hardening rate) and in compression testing (due to work softening)

Materials that undergo severe work softening are prone to compressive instabilities. While useful in itself, this precludes measurement of the bulk plastic deformation behavior of the material, just as the necking instability in tension testing prevents measurement of plastic deformation behavior at large strains. Several metallurgical conditions can lead to such work softening. These include dynamic recovery and dynamic recrystallization where substructure rearrangements and dislocation reductions lead to a rapid decrease in flow stress. Morphological changes in second phases, such as the rapid spheroidization of pearlite at elevated temperatures, the coarsening of small spherical precipitates, and the coarsening of martensitic substructures, are another source of work softening. Further examples of work softening include incipient melting of eutectic phases and localized shear-band formation, seen commonly in titanium alloys.

Reference cited in this section

12. J.J. Jonas and M.J. Luton, Flow Softening at Elevated Temperatures, *Advances in Deformation Processing*, J.J. Burke and V. Weiss, Ed., Plenum, 1978, p 238

Uniaxial Compression Testing

Howard A. Kuhn, Concurrent Technologies Corporation

Test Methods

Axial compression testing is a useful procedure for measuring the plastic flow behavior and ductile fracture limits of a material. Measuring the plastic flow behavior requires frictionless (homogenous compression) test conditions, while measuring ductile fracture limits takes advantage of the barrel formation and controlled stress and strain conditions at the equator of the barreled surface when compression is carried out with friction. Axial compression testing is also useful for measurement of elastic and compressive fracture properties of brittle materials or low-ductility materials. In any case, the use of specimens having large L/D ratios should be avoided to prevent buckling and shearing modes of deformation.

Axial compression tests for determining the stress-strain behavior of metallic materials are conducted by techniques described in test standards, such as:

- ASTM E 9, "Compression Testing of Metallic Materials at Room Temperature"
- DIN 50106, "Compression Test, Testing of Metallic Materials"
- ASTM E 209, "Compression Tests of Metallic Materials at Elevated Temperatures with Conventional or Rapid Heating Rates and Strain Rates"

This section briefly reviews the factors that influence the generation of valid test data for tests conducted in accordance with ASTM E 9 and the capabilities of conventional universal testing machines (UTMs) for compression testing.

Specimen Buckling

As previously noted, errors in compressive stress-strain data can occur by the nonuniform stress and strain distributions from specimen buckling and barreling. Buckling can be prevented by avoiding the use of specimens with large length-to-diameter ratios, L/D. In addition, the risk of specimen buckling can be reduced by careful attention to alignment of the loading train and by careful manufacture of the specimen according to the specifications of flatness, parallelism, and perpendicularity given in ASTM E 9. However, even with well-made specimens tested in a carefully aligned loading train, buckling may still occur. Conditions that typically induce buckling are discussed in the following sections.

Alignment. The loading train, including the loading faces, must maintain initial alignment throughout the entire loading process. Alignment, parallelism, and perpendicularity tests should be conducted at maximum load conditions of the testing apparatus.

Specimen Tolerances. The tolerances given in ASTM E 9 for specimen end-flatness, end-parallelism, and end-perpendicularity should be considered as upper limits. This is also true for concentricity of outer surfaces in cylindrical specimens and uniformity of dimensions in rectangular sheet specimens. If tolerances are reduced from these values, the risk of premature buckling is also reduced.

Inelastic Buckling. Only elastic buckling is discussed in ASTM E 9. This may be somewhat unrealistic, because for the most slender specimen recommended, the calculated elastic buckling stresses are higher than can be achieved in a test. This specimen has a length-to-diameter ratio of 10. An approximate calculation using the elastic Euler equation for a steel specimen with flat ends on a flat surface (assumed value of end-fixity coefficient is 3.5) yields a buckling stress in excess of 4100 MPa (600 ksi); the comparable value for an aluminum specimen would be 1380 MPa (200 ksi). These values, however, are not realistic.

Buckling stress in the above example should not be calculated by an elastic formula but by an inelastic buckling relation. In terms of inelastic buckling it has been concluded that the following relation appropriately calculates inelastic buckling stresses (Ref 13):

$$S_{cr} = C\pi^2 \left[\frac{E_t}{(L/\rho)^2} \right] \qquad \text{(Eq 5)}$$

where S_{cr} is the buckling stress in MPa (ksi); C is the end-fixity coefficient; E_t is the tangent modulus of the stress-strain curve in MPa (ksi); L is the specimen length in mm (in.); and r is the radius of gyration of specimen cross section in mm (in.). Equation 1 reduces to the Euler equation if E, the modulus of elasticity, is substituted for E_t.

Rearranging Eq 5 to combine the stress-related factors results in:

$$\left(\frac{1}{C\pi^2} \right) \left(\frac{L}{\rho} \right)^2 = \frac{E_t}{S_{cr}} \qquad \text{(Eq 6)}$$

Note that the value of the right side of Eq 6 decreases as stress increases in a stress-strain curve. In a material with an elastic-pure-plastic response, the right side of Eq 6 vanishes, because E_t becomes zero, and buckling will always occur at the yield stress. When the material exhibits strain hardening, calculations using Eq 6 will yield the appropriate specimen dimensions to resist buckling for given values of stress.

Side Slip. Figure 10 illustrates one form of buckling of cylindrical specimens that can result from misalignment of the loading train under load or from loose tolerances on specimen dimensions. The ends of the specimen undergo sideslip, resulting in a sigmoidal central axis. This form of buckling could be described by Eq 5 and 6, provided an appropriate value of the end-fixity coefficient can be assigned.

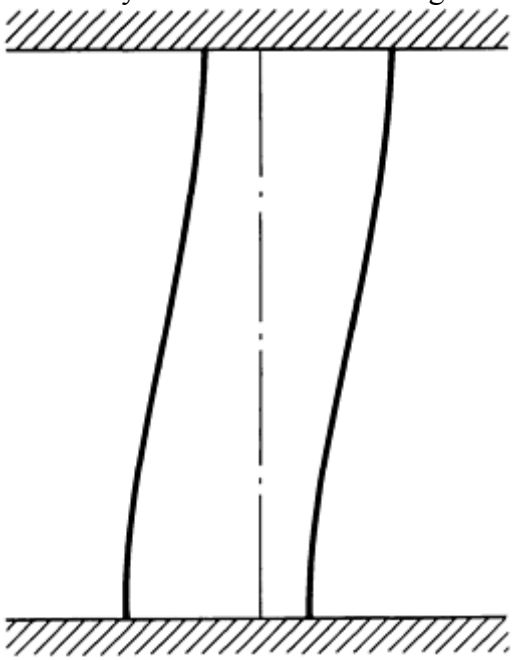

Fig. 10 Schematic diagram of side-slip buckling. The original position of the specimen centerline is indicated by the dashed line.

Thin-Sheet Specimens. In testing thin sheet in a compression jig, approximately 2% of the specimen length protrudes from the jig. Buckling of this unsupported length can occur if there is misalignment of the loading train such that it does not remain coaxial with the specimen throughout the test (Ref 14). A typical compression jig and contact-point compressometer are shown in Fig. 11(a) and (b) respectively.

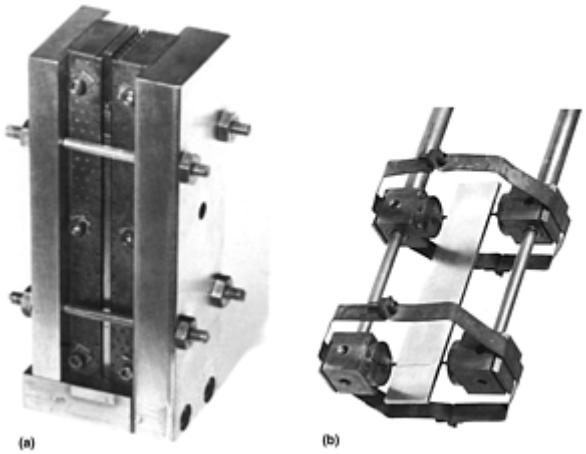

Fig. 11 Compression testing of thin-sheet specimens. (a) Sheet compression jig suitable for room-temperature or elevated-temperature testing. (b) Contact-point compressometer installed on specimen removed from jig. Contact points fit in predrilled shallow holes in the edge of the specimen.

Barreling of Cylindrical Specimens

When a cylindrical specimen is compressed, Poisson expansion occurs. If this expansion is restrained by friction at the loading faces of the specimen, nonuniform states of stress and strain occur as the specimen acquires a barreled shape (Fig. 12). The effect on the stress and strain distributions is of consequence only when the deformations are on the order of 10% or more.

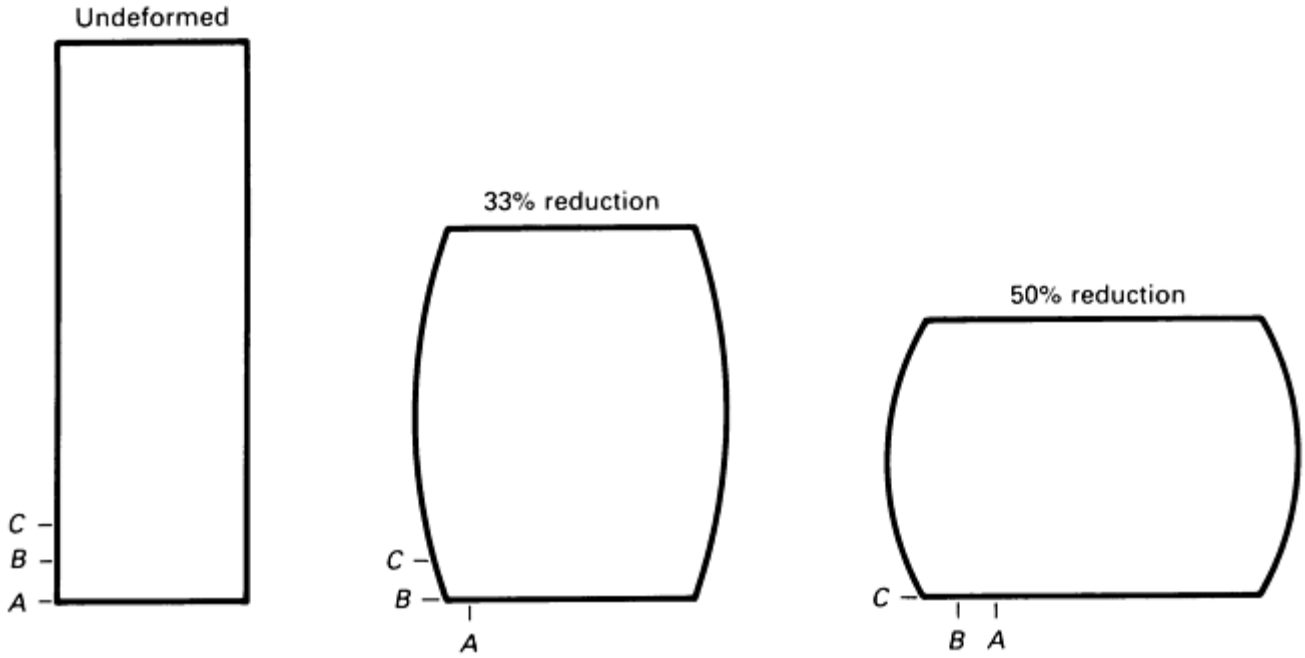

Fig. 12 Barreling during a test when the friction coefficient is 1.00 at the specimen loading face. Note that as the deformation increase, points *A*, *B*, and *C* originally on the specimen sides, move to the loading face.

Friction on the loading face causes rollover. As shown in Fig. 12, points originally on the sides of the specimen are ultimately located on the specimen end face. Use of a high-pressure lubricant at the loading surface of the specimen reduces friction. One such material commonly used is 0.1 mm (0.004 in.) thick Teflon sheet. The action of the lubricant may be enhanced if the bearing surfaces that apply the load are hard and highly polished. The use of tungsten-carbide bearing blocks is recommended for all materials undergoing compression testing. Other techniques have been used to reduce nonuniformity of stress and strain distributions along the gage length (Ref 15, 16).

The contact area between the lateral faces of the specimen and the lateral support guides of the testing jig must be well lubricated. Personnel engaged in sheet compression testing should become familiar with the literature on the subject. A selected bibliography on this subject is given in ASTM E 9.

Testing Machine Capacity

In a compression test performed to large strains (e.g., to obtain fracture data), a large load capacity may be required. For example, consider four medium-length cylindrical specimens suggested in ASTM E 9, where specimens are specified with diameters that range from 12.7 to 28.4 mm (0.50 to 1.12 in.) and with length-to-diameter ratios of 3. Using these specimen sizes, consider the testing of a material with a yield stress of 1380 MPa (200 ksi) and a compression strain-hardening exponent of 0.05. Figure 13 illustrates the load-capacity requirements to reach a height reduction of 60% for each of the four cylinders recommended in ASTM E 9. The maximum required load is approximately 3.5 times the load at yield. The required capacity for testing the same specimens to failure at 60% strain in tension would be no more than 1.5 times the yield loads.

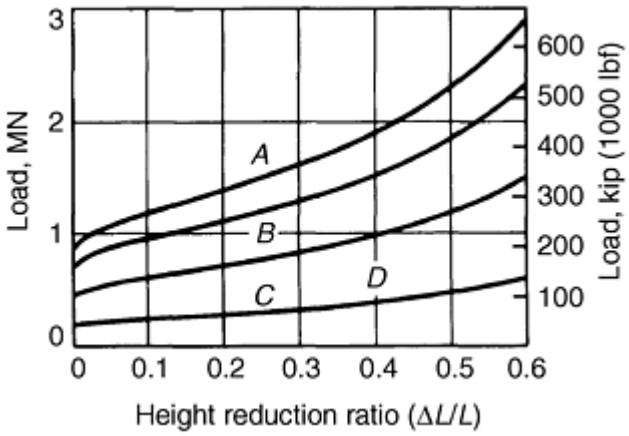

Fig. 13 Load requirements for compressing specimens of various diameters made of a material with a yield stress of 1380 MPa (200 ksi) and a strain-hardening exponent of 0.05. Diameters: *A* = 28.4 mm (1.12 in.), *B* = 25.4 mm (1.00 in.), *C* = 20.3 mm (0.80 in.), *D* = 12.7 mm (0.50 in.). Length-to-diameter ratio (*L*/*D*) = 3

Medium-Strain-Rate Testing

Medium-strain-rate compression testing with conventional load frames is very similar to low-strain-rate compression testing. For medium-rate testing, the load frames require the capability to generate higher crosshead or ram velocities. An important consideration is the stiffness of the machine, as discussed in more detail in the article "Testing Machines and Strain Sensors" in this Volume. For tests at a uniform strain rate, a high machine stiffness is desired; techniques to increase the stiffness of a hydraulic machine are described in Ref 17. This section describes some of the techniques used to obtain medium strain rates with conventional test frames and additional experimental factors for measurement of load and strain at medium rates.

Grip design for compression testing at medium strain rates requires the same considerations that apply to grip design for low strain rates. The compression specimen typically is sandwiched between two hard, polished platens that are placed in a subpress designed to maintain parallel faces during deformation. A typical grip assembly is shown in Fig. 14, in which a compression specimen (5.1 mm, or 0.2 in., long by 5.1 mm, or 0.2 in., diam) is in place and ready for testing. The ram is shown in position and is separated from the subpress by approximately 20 mm (0.8 in.). This gap allows time (approximately 2 ms at the highest ram velocity) for the ram to accelerate to the specified velocity. In this test, the stroke of the ram must be set accurately to ensure the desired deformation.

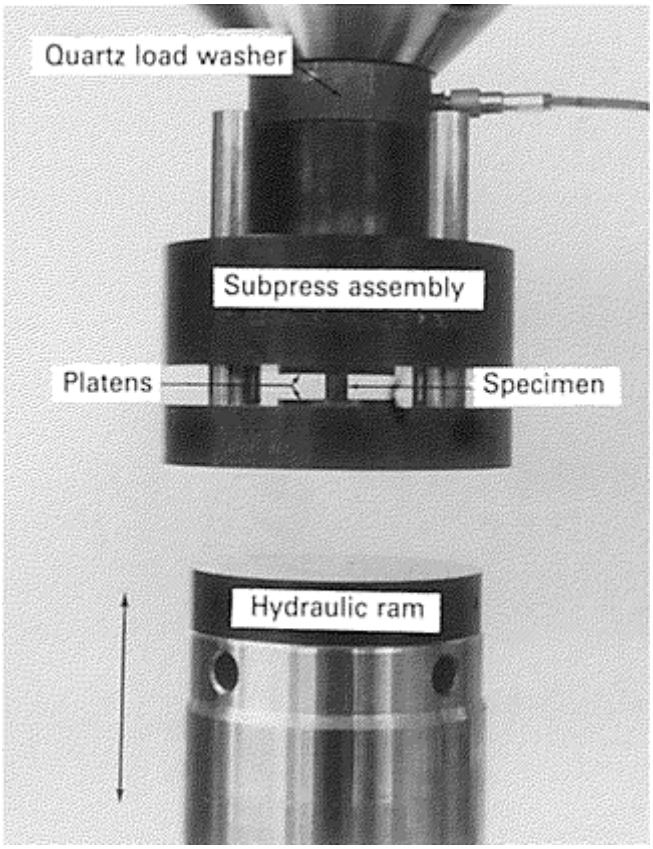

Fig. 14 Subpress assembly for medium strain-rate testing with conventional load frame. The specimen, which is 5.1 mm (0.2 in.) diam by 5.1 mm (0.2 in.) long, is sandwiched between two highly polished platens. A quartz load washer is shown positioned above the subpress assembly.

Measurement of Load and Displacement. As the strain rate increases, the measurement of load and displacement becomes increasingly more difficult. The requirement for adequate frequency response in the signal conditioners and the problems associated with load-cell ringing were discussed in the introduction to this article. In this section, the measurement of load and displacement at medium strain rates is described in more detail.

Measurement of Load. A typical load cell determines load by measuring displacement in an elastic member, such as a diaphragm or cylinder. The displacements are measured with bonded strain gages; this gives the load cell sufficient intrinsic frequency response for testing at medium strain rates. However, a problem often arises due to ringing in the load cell. The load cell has a natural frequency of vibration determined by geometry and physical properties, such as density and elastic modulus. Typical load cells have a natural frequency in the range of 500 to 5000 Hz. In effect, the natural frequency of vibration sets the bandwidth of the load-measuring system.

By this criterion alone, load cells should be sufficient for compression testing at strain rates as high as 100 s^{-1}. However, the transient response of the load cell in practice limits the measurement to much lower strain rates. When a constant-strain-rate test is desired, deformation must be initiated by an impact due to the acceleration time required by the ram. This impact can excite the natural vibrational mode of the load cell, which will produce oscillations in the output signal that can mask the actual load measurement. Unless the impact is dampened by some means, load measurement at strain rates greater than about 1 s^{-1} can be subject to load-cell ringing.

Ringing of the load cell can be minimized by selecting a load cell with a high vibrational frequency. If the natural frequency is sufficiently high, the vibrational mode may not be excited by the impact, or if excited, it may be possible to remove it from the signal with a low pass filter. Another method to reduce ringing is to dampen the impact that initiates deformation within the specimen. Often, a thin layer of deformable material placed between the impacting surfaces is sufficient to remove the higher frequencies generated by the impact that can excite the natural frequency of the load cell. For example, in the configuration shown in Fig. 14, a single loop, approximately 50 mm (2 in.) in diameter, of 0.51 mm (0.02 in.) diameter lead-tin solder wire

placed on the impacting face of the hydraulic ram was found to be effective in minimizing load-cell ringing. Such layers, however, may complicate measurement of displacement within the specimen.

At strain rates close to 100 s^{-1}, the standard load cell either may not possess the necessary frequency response, or it may ring excessively. These characteristics can make the load cell inadequate for load measurement. Under these conditions, a quartz piezoelectric device, such as a load washer (Fig. 14), is useful. The load washer is convenient because it is easily adapted to a compression test; it also has excellent intrinsic frequency response and a high fundamental vibrational frequency. However, these devices require special signal conditioning and low-capacitance cables.

Measurement of Strain. The direct measurement of strain at medium strain rates presents a challenge. Many of the devices typically used for low-strain-rate testing are inappropriate at medium strain rates. Extensometers, for example, may have the necessary response characteristics for medium-strain-rate testing. However, it is difficult to ensure that the rapid and large displacement in small compression specimens will not damage the fragile extensometer.

Many hydraulic test frames use a linear variable differential transformer (LVDT) to control the motion of the hydraulic ram. This LVDT signal is comprised of displacements within the specimen as well as elastic displacements throughout the test frame. To relate this signal to displacements within the specimen, the latter contribution must be subtracted; this problem also is encountered at low strain rates. If a deformable material is placed between the impact surfaces to dampen the impact, the displacements within this layer also must be subtracted from the LVDT signal.

A common practice is to mount the LVDT at an off-axis position adjacent to the specimen. The benefit of this configuration is that a displacement measurement is possible between two points that are quite close to the specimen; this measurement includes less of the elastic deformation in the load frame. When a measurement is made at an off-axis position, it is important to verify that the measurement truly represents displacements within the sample. Often, two LVDT units are mounted at diametrically opposite positions, and their outputs are processed to eliminate the effects of nonplanar motion. The LVDT suffers from an intrinsic frequency-response limitation determined by the excitation frequency. Standard excitation frequencies are in the range of 1 to 5 kHz, which limits the frequency response to around 100 to 500 Hz.

Velocity transducers, which have good intrinsic frequency response, have been used to measure the motion of the specimen and grip assembly (Ref 17). Their output can be integrated electronically or by computer to obtain the displacement. Generally, these also require mounting at off-axis locations.

Strain measurement by noncontact methods is becoming more common with optical extensometers or laser interferometers. Laser interferometers, which are capable of operating at high sampling rates, can be used to measure strain at strain rates exceeding 10^3 s^{-1}.

Types of Compressive Fracture

For all but the most ductile materials, cylindrical specimens develop cracks when they are compressed. The cracks generally initiate on the outer surface of the compressed specimen. As the specimen is further deformed, the initiated cracks propagate, and new cracks form. Some different modes of compression fracture are described in Ref 18 and some examples are described in the following sections.

Orange Peel Cracking. In many materials, roughening or wrinkling of the surface (orange peel effect) occurs prior to compressive cracking. This effect is particularly prominent in some aluminum alloys. An extreme example is illustrated for an aluminum alloy 7075-T6 specimen in Fig. 15. The specimen is shown after 72% deformation. Wrinkling first appeared at 10 to 15% compressive deformation, and macrocracking occurred after 50 to 60% deformation. Microscopic examination revealed many microcracks in the valleys of the wrinkles, with greatest concentration in the equatorial region of the specimen. Defining a compression strength or a strain criterion of fracture would be difficult for this material.

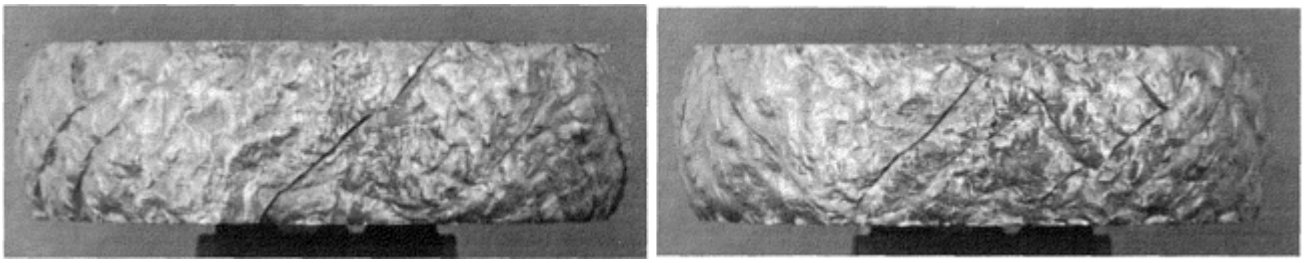

Fig. 15 Two views of a 72% compressed specimen of aluminum alloy 7075-T6 displaying orange peel effect. The loading axis is vertical. Extensive macrocracking is evident in the severely wrinkled surface. Microscopic examination of the surface revealed extensive microcracking in the valleys of the wrinkles. Source: Ref 16

Macrocracks in Steel. A case in which macrocracks form without apparent precursor microcracks is shown in Fig. 16. The material is AISI-SAE 4340 steel tempered at 204 °C (400 °F), yielding a hardness of 52 HRC. The cracks initiated one at a time and extended across the surface of the specimen almost instantaneously. The first cracks appeared when the compressive deformation reached 30%, and other cracks continued to initiate until the test was concluded at 72% deformation, which is the condition shown in Fig. 16. The specimen was still intact, and subsequent sectioning revealed that the cracks penetrated inward a distance of diameter.

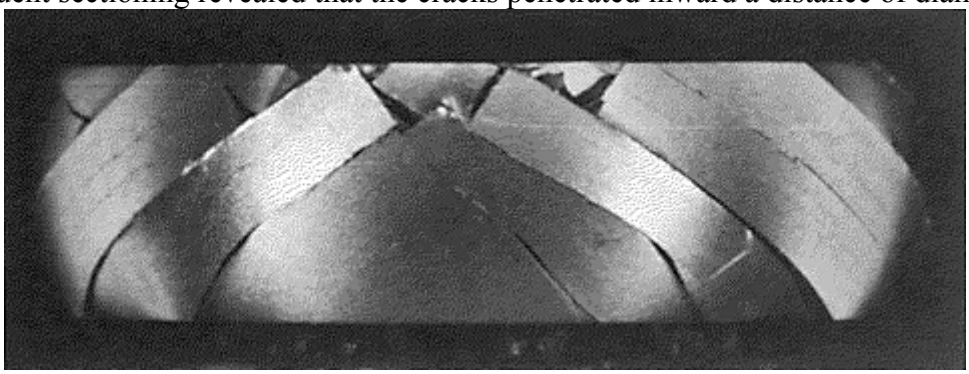

Fig. 16 Shear cracks in a 72% compressed specimen of AISI-SAE 4340 steel. The cracks initiated one at a time, starting when the deformation was 30%. Source: Ref 16

Microcrack to Macrocrack Coalescence. In some tungsten alloys, the first visible evidence of fracture is a shear macrocrack that appears at the equator of the specimen after 45 to 50% compressive deformation. However, using fluorescent-dye penetrant methods, microcrack initiation was detected at 25% deformation (Ref 18). For this material, if crack initiation is the criterion of failure, it is necessary to state the method of crack detection with the selected parameter for strength.

References cited in this section

13. G. Gerard, *Introduction to Structural Stability Theory*, McGraw-Hill, 1962, p 19–29

14. R. Papirno and G. Gerard, "Compression Testing of Sheet Materials at Elevated Temperatures," *Elevated Compression Testing of Sheet Materials*, STP 303, ASTM, 1962, p 12–31

15. T.C. Hsu, A Study of the Compression Test for Ductile Materials, *Mater. Res. Stand*., Vol 9 (No. 12), Dec 1969, p 20

16. R. Chait and C.H. Curll, "Evaluating Engineering Alloys in Compression," *Recent Developments in Mechanical Testing*, STP 608, ASTM, 1976, p 3–19

17. R.H. Cooper and J.D. Campbell, Testing of Materials at Medium Rates of Strain, *J. Mech. Eng. Sci*., Vol 9, 1967, p 278

18. R. Papirno, J.F. Mescall, and A.M. Hansen, "Fracture in Axial Compression of Cylinders," *Compression Testing of Homogeneous Materials and Composites*, R. Chait and R. Papirno, Ed., STP 808, ASTM, 1983, p 40–63

Acknowledgments

Portions of this article were adapted from R. Papirno, Axial Compression Testing (p 55–58) and P.S. Follansbee and P.E. Armstrong, Compression Testing by Conventional Load Frames at Medium Strain Rates (p 192–193) in *Mechanical Testing,* Vol 8, *ASM Handbook,* ASM International, 1985.

Uniaxial Compression Testing

Howard A. Kuhn, Concurrent Technologies Corporation

References

1. T. Erturk, W.L. Otto, and H.A. Kuhn, Anisotropy of Ductile Fracture—An Application of the Upset Test, *Metall. Trans*., Vol 5, 1974, p 1883
2. W.A. Kawahara, Tensile and Compressive Materials Testing with Sub-Sized Specimens, *Exp. Tech*., Nov/Dec, 1990, p 27–29
3. W.A. Backofen, *Deformation Processing*, Addison-Wesley, Reading, MA, p 53
4. J.H. Faupel and F.E. Fisher, *Engineering Design*, John Wiley & Sons, 1981, p 566–592
5. G.E. Dieter, *Mechanical Metallurgy*, 2nd ed., McGraw-Hill, 1976, p 561–565
6. G.E. Dieter, Evaluation of Workability: Introduction, *Forming and Forging*, Vol 14, *ASM Handbook,* ASM International, 1988, p 365
7. J.E. Hockett, The Cam Plastometer, in *Mechanical Testing*, Vol 8, *ASM Handbook*, ASM International, 1985, p 197
8. R. Herbertz and H. Wiegels, Ein Verfahren Zur Verwirklichurg des Reibungsfreien Zylinderstanch versuchs für die Ermittlung von Fliesscurven, *Stahl Eisen*, Vol 101, 1981, p 89–92
9. K. Lintermanns Fander, "The Flow and Fracture of Al-High Mg-Mn Alloys at High Temperatures and Strain Rates," Ph.D. dissertation, University of Pittsburgh, 1984, p 258
10. H.A. Kuhn, P.W. Lee, and T. Erturk, A Fracture Criterion for Cold Forging, *J. Eng. Mater. Technol. (Trans. ASME)*, Vol 95, 1973, p 213–218
11. H.A. Kuhn, Workability Theory and Application in Bulk Forming Processes, *Forming and Forging*, Vol 14, *ASM Handbook*, ASM International, 1988, p 389–391
12. J.J. Jonas and M.J. Luton, Flow Softening at Elevated Temperatures, *Advances in Deformation Processing*, J.J. Burke and V. Weiss, Ed., Plenum, 1978, p 238